EurJOC European Journal of Organic Chemistry

FULL PAPER

DOI: 10.1002/ejoc.201200438

Seven-Membered Intramolecular Hydrogen Bonding of Phenols: Database Analysis and Phloroglucinol Model Compounds

Ronald K. Castellano,*[a] Yan Li,[a] Edwin A. Homan,[a] Andrew J. Lampkins,[a] Iris V. Marín,[a] and Khalil A. Abboud[a]

Dedicated to Professor François Diederich on the occasion of his 60th birthday

Keywords: Conformation analysis / Crystal engineering / Hydrogen bonds / Solid-state structures / Supramolecular chemistry

Seven-membered intramolecular hydrogen bonding (7MHB) arrangements involving phenolic hydroxyl group donors have been investigated through Cambridge Structural Database (CSD) and literature mining, and by the characterization of model compounds. The CSD reveals the numerous H-bond accepting functional groups that can participate in 7MHB when they are proximal to a phenolic OH, including alcohols, amides, amines, ethers, N-containing heterocycles, ketones, *N*-oxides, phosphates, and phosphane oxides. The HB contacts are defined by $O_{phenol}\cdots N$ and $O_{phenol}\cdots O$ distances of ca. 2.7 Å, and two dihedral angles that fall within the range of typical peptide γ-turns. Two of the identified 7MHB motifs have been readily mapped onto the phloroglucinol (1,3,5-trihydroxybenzene) scaffold to provide eight model compounds; intramolecular hydrogen bonding involving all three hydroxyl groups is shown to persist in solution and the solid state for the compounds. Intramolecular 7MHB enforces nonplanar conformations that should be useful when designing molecular hosts and catalysts.

Introduction

Intramolecular hydrogen bonding (H-bonding) is a central strategy to preorganize otherwise flexible molecules into "functional" conformations. Classic examples come from peptides, in which secondary structures − helices, turns, and sheets − arise from geometrically well-defined H-bonding interactions between intrachain amino acids.[1] Relevant in this context are γ-turns, seven-membered H-bonding (7MHB) arrangements between amide C=O acceptors and N–H donors on i and i + 2 residues.[1a–1d] Although well-studied through model systems and peptidomimetics,[2] these interactions are rarely considered for controlling the conformation/shape of synthetic molecules given their "weakness" relative to five- and six-membered motifs.[3] Indeed, only a small amount of **1** is in the "folded" form in dilute dichloromethane solution at room temperature, whereas **2** is predominantly hydrogen bonded under the same conditions (Figure 1, a).[2a]

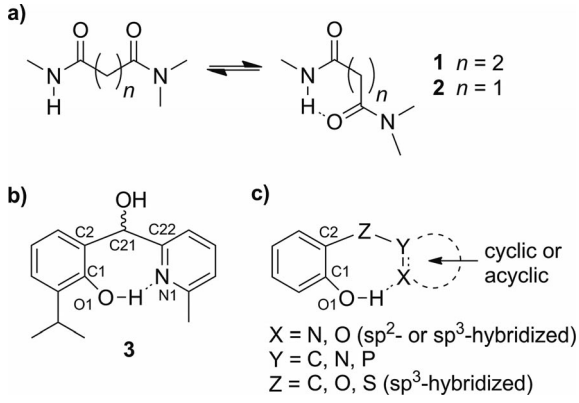

Figure 1. Intramolecular seven-membered hydrogen-bonding (7MHB) in (a) acyclic amides **1** and **2** (see ref.[2a]) and (b) a β-turn mimetic **3** (see ref.[4]). (c) A general approach to achieve persistent 7MHB involving phenols, confirmed through crystallographic database searching and model compound investigations.

In 1999, Koskinen and co-workers demonstrated robust 7MHB by employing a stronger H-bond donor, phenol, and stronger H-bond acceptor, pyridine (Figure 1, b).[4] Molecule **3**, for example, is accordingly almost fully H-bonded in organic solution (e.g., CCl_4) at 295 K, and the geometric parameters describing the stabilized conformation (based on X-ray analysis) closely mimic classic peptide γ-turns. For

[a] Department of Chemistry, University of Florida, P. O. Box 117200, Gainesville, FL 32611, USA
Fax: +1-352-846-0296
E-mail: castellano@chem.ufl.edu
Homepage: http://www.chem.ufl.edu/~castellano/

Supporting information for this article is available on the WWW under http://dx.doi.org/10.1002/ejoc.201200438.

3, this includes the values for the two relevant torsion angles [C1–C2–C21–C22 –80.3(4)°; C2–C21–C22–N1 +62.7(4)°] and the O1···N1 H-bond length [2.702(4) Å]. Although not systematically considered to date, the Koskinen work speaks to a general recipe for engineering 7MHB motifs with phenols (Figure 1, c); any reasonable H-bond acceptor

Table 1. Representative 7MHB patterns identified from the CSD where X = N, O (sp^2-hybridized) and Z = C or O (sp^3-hybridized).[a]

Entry	X[b]	CSD code	Ref.	Chemical structure	X-ray structure[c]	O1···X [Å][d]	C1–C2–Z–Y [°][d]	C2–Z–Y–X [°][d]
1	N (pyridine)	CIVZUD	[6]	**3**		2.6914(13)	–73.0	+57.7
		HOVHAB	[4]			**2.702(4)**	**–80.3(4)**	**+62.7(4)**
		HOVHEF	[4]			2.690(4)	+71.8(4)	–65.3(4)
2	N (imidazole)	**NEYWIY**	[7]			**2.62**	**–64.6**	**+66.0**
3	N (pyrazole)	**ENISID**	[8]			**2.769(4)**	**+72.9**	**–80.4**
		FOMGUK	[9]			2.6846(18)	+65.1	–61.4
		OHAXOK	[10]			2.64	+59.9	–60.3
		TIXSOJ	[11]			2.65	–56.3	+60.8
4	N (1,2,4-triazole)	**JITTEM**	[12]			**2.965(3)**	**–78.0**	**+71.0**
		LIKBUD	[13]			2.88	+79.2	–66.2
		POCPUT	[14]			2.807(4)	–69.5	+74.6
		POCQII	[14]			2.75	–71.2	+69.0
5	O (amide)	SAVXUJ	[15]			2.66	+69.3	–57.0
		XICBUG	[16]			2.558(4)	–67.4	+39.1
		XICCAN	[16]			**2.547(1)**	**–64.7**	**+48.0**
6	O (ketone)	**NOKLAB**	[17]			**2.83**	**+85.5**	**–88.6**
		PEKBAI	[18]			2.69	+47.1	–43.8
		SIVXIE	[19]			2.68	+51.3	–38.3
		YOQVAC	[20]			2.66[e]	–50.2[e]	+43.5[e]
		YOQVEG	[20]			2.63[e]	+51.6[e]	–38.3[e]
7	O (phosphate)	**OQUNPR**	[21]			**2.635(6)**	**–58.6**	**65.9**
8	O (phosphane oxide)	JEWHOJ	[22]			2.63	–66.4	+53.7
		JEWHUP	[22]			2.70[e]	–71.7[e]	+60.5[e]
		JEWJAX	[22]			2.64[e]	–64.3[e]	+43.0[e]
		QELROP	[23]			**2.646(1)**	**+74.3**	**–50.5**

[a] Structures were obtained from the CSD, version 5.31 (August 2010). In all cases, $R \leq 0.10$. Bold-faced data corresponds to the chemical and X-ray structures drawn (the remaining chemical and X-ray structures can be found in the Supporting Information). In all cases, the measurements for only one unique molecule from the unit cell are given. The hybridization designation is approximate and for classification purposes only. [b] See Figure 1 for the definition of X. [c] X-ray structure coordinate files were exported from the CSD as CIF files and processed for visualization using Accelyrs Discovery Studio Visualizer. H-bonds are shown as dashed lines and selected atoms (including most H atoms) have been omitted for clarity. Atom colors: C, gray; Cu, pink; H, white; N, blue; O, red; P, orange. [d] Distances with errors have been taken from the original literature citations. Otherwise, measurements were made within Accelyrs Discovery Studio Visualizer. [e] Average values for two symmetry nonequivalent 7MHB motifs within one molecule.

in the position X of the framework shown should stabilize a H-bonded conformation that closely approximates a γ-turn (provided a suitable hinge point Z is present).

Reported here are the results of both a Cambridge Structural Database (CSD) search and a model compound investigation that reveal the structural and spectroscopic consequences of 7MHB involving phenols. CSD examples show how the structural paradigm shown in Figure 1 (c) is satisfied by a wide range of H-bond accepting functional groups proximal to the phenol, including alcohols, amides, amines, ethers, N-containing heterocycles (e.g., imidazole, pyrazole, pyridine, and triazole), ketones, *N*-oxides, phosphates, and phosphane oxides. To further show how these patterns are persistent in both solution and the solid state in the context of *designed* molecules, we have extended two of them to the phloroglucinol (1,3,5-trihydroxybenzene) platform. The choice of scaffold draws on our experience in preparing per-substituted phloroglucinols,[5] and provides access to dynamic molecules that can adopt bowl shapes that are considered attractive for applications in molecular recognition and catalysis.

Results and Discussion

Representative CSD and Literature Search Results

Provided in Table 1 are eight representative 7MHB motifs (25 total examples) for cases in which X is an sp^2-hybridized nitrogen or oxygen atom and Z is an sp^3-hybridized hinge atom (C or O). All feature a relatively short O1···X H-bond length (average 2.69 Å) and similar dihedral angle values, particularly within motif classes. Table 1, entry 1 showcases the Koskinen pyridine H-bond acceptor motif,[4] whereas entries 2, 3, and 4 show that 7MHB is similarly compatible with five-membered heterocycles including imidazole, pyrazole, and 1,2,4-triazole. Cases for which Y = N, represented by the pyrazoles (Table 1, entry 3), are particularly accessible synthetically through routine substitution chemistry involving 2-halomethyl phenols (see below). No examples of 7MHB involving 1,2,3-triazoles emerged from the search, although these motifs are, in principle, accessible through copper-catalyzed Huisgen cycloaddition chemistry.[36] Table 1, entries 5–8 demonstrate how the sp^2-hybridized oxygen of C=O and P=O bonds can also serve as H-bond acceptors for phenol OH donors. As with the pyrazoles, amide-functionalized phenols (Table 1, entry 5) are quite easily prepared and can be considered for designed molecules (see below).

Provided in Table 2 are two representative 7MHB motifs (5 total examples) for cases in which X is an sp^3-hybridized nitrogen (of an amine) or oxygen atom (of an alcohol or ether) and Z is an sp^3-hybridized hinge atom (C or O). The average O1···X(sp^3) H-bond length, 2.66 Å, compares favorably to the average O1···X(sp^2) value give in Table 1 (2.69 Å). The dihedral angle values for C1–C2–Z–Y and C2–Z–Y–X nicely accommodate the 7MHB arrangement, and are enforced in many cases through polycyclic arrangements. HAGGIF (Table 2, entry 2) is one exception, featuring an H-bond interaction between the phenolic OH and the hydroxyl oxygen of a flexible 1-hydroxypropan-2-yl side chain at C2. The chemical and X-ray structures not shown graphically in Tables 1 and 2 can be found in the Supporting Information.

While trends relating O1···X H-bond length to H-bond (acceptor) strength (as it varies with functional group) are difficult to discern from the crystallographic data presented in Tables 1 and 2, relative H-bond strength can be inferred from the ^{1}H NMR spectroscopic data available in the literature (Table 3). Data shown comes from a commonly used H-bond compatible solvent ($CDCl_3$). All compounds capable of 7MHB show downfield shifts of the phenolic OH resonance (δ_{OH}) by 3.6–7.9 ppm ($\Delta\delta_{OH}$) relative to mono-

Table 2. Representative 7MHB patterns identified from the CSD where X = N, O (sp^3-hybridized) and Z = C or O (sp^3-hybridized).[a]

Entry	X[b]	CSD code	Ref.	Structure	X-ray structure[c]	O1···X [Å] [d]	C1–C2–Z–Y [°][d]	C2–Z–Y–X [°][d]
1	N (amine)	CAPHAD	[24]	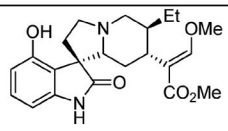	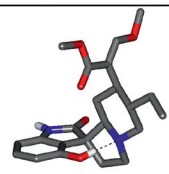	2.60	+3.72	–54.8
		NIFDUB	[25]			**2.613(10)**	**–54.7**	**+81.3**
2	O (ether or alcohol)	**HAGGIF**	[26]	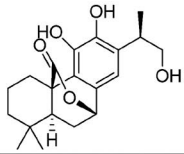	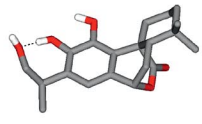	**2.541(3)**	**–88.4**	**+71.8**
		RIJNUT	[27]			2.86	+68.6	–87.2
		XORZUZ	[28]			2.704(3)	+85.2	–66.4

[a] Structures were obtained from the CSD, version 5.31 (August 2010). In all cases, $R \leq 0.10$. Bold-faced data corresponds to the chemical and X-ray structures drawn (the remaining chemical and X-ray structures can be found in the Supporting Information). In all cases, the measurements for only one unique molecule from the unit cell are given. The hybridization designation is approximate and for classification purposes only. [b] See Figure 1 for the definition of X. [c] X-ray structure coordinate files were exported from the CSD as CIF files and processed for visualization using Accelyrs Discovery Studio Visualizer. H-bonds are shown as dashed lines and selected atoms (including most H atoms) have been omitted for clarity. Atom colors: C, gray; H, white; N, blue; O, red. [d] Distances with errors have been taken from the original literature citation. Otherwise, measurements were made within Accelyrs Discovery Studio Visualizer.

meric 2-isopropylphenol[4] (δ = 4.7 ppm). The chemical shifts respond logically to H-bond acceptor strength (basicity). Table 3, entries 2–4, for example, show decreasing δ_{OH} values in response to decreasing nitrogen basicity; from pyridine (pK_a (conjugate acid) = 5.2), to pyrazole (pK_a 2.5), to 1,2,4-triazole (pK_a = 2.3).[37] As the acceptor atom basicity decreases, from an aliphatic amine (Table 3, entry 8), to an aliphatic amide (entry 5), to an aliphatic ketone (entry 6), δ_{OH} shifts upfield as the H-bond strength accordingly decreases. For aryl ketones (Table 3, entry 6), a methoxy substituent in the *para* position, as expected, increases δ_{OH} (the H-bonding contact is enhanced) relative to the unsubstituted phenyl ketone [compare the pK_{HB} values of acetophenone (1.11) and *p*-methoxyacetophenone (1.33)[38]]. Although phenol-based 7MHB interactions are commonly overlooked in the literature (in fact, the OH chemical shift is often not reported or assigned), they are easily identifiable on the basis of ^{1}H NMR spectroscopic data obtained in nonpolar solvents (e.g., $CDCl_3$).

Table 3. Representative ^{1}H NMR spectroscopic data (δ_{OH}, $CDCl_3$) for the 7MHB motifs presented in Tables 1 and 2 (literature values).[a]

Entry	Molecular example	δ_{OH} ($CDCl_3$) [ppm]	δ_{OH} ($CDCl_3$) [ppm], related molecules[b]
1	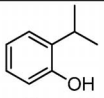	4.7[4]	–
2	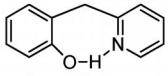	11.7[4]	10.1,[29] 10.2,[29] 10.9,[4] 11.2,[4] 12.04[]
3	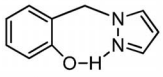	10.3[30]	9.97,[31] 10.9,[11] and this work
4	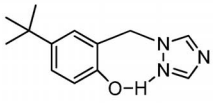	9.23[12]	–
5	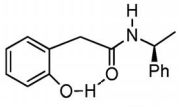	9.87[32]	this work
6	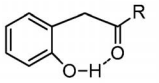	R = Me: 7.20[33] R = Ph: 7.63[33] R = *p*-MeOPh: 8.20[33]	7.0–8.2 (8 other examples)[33]
7	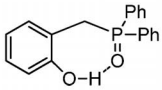	9.87[34]	8.29,[22] 9.76[23]
8	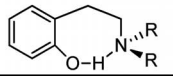	R = (*S*)-CHMePh: 11.9[35]	–

[a] Standard ^{1}H NMR solution concentrations and ambient temperature are assumed. δ_{OH} values, in many cases, have been inferred from the reported ^{1}H NMR spectroscopic data and specific chemical structures. [b] The specific molecular structures can be found in the corresponding citations. Excluded are cases for which the O1···X interaction is influenced by a favorably constrained molecular structure.

Phloroglucinol Model Compounds; General Design

To complement the literature analysis described above, we have selected two of the intramolecular 7MHB motifs from Table 1 to map onto a synthetic platform, phloroglucinol (1,3,5-trihydroxybenzene) (Figure 2, a), for studies in both solution and the solid state. The general design is inspired by the rich literature that has employed C_3-symmetric persubstituted benzenes for host–guest studies and catalysis.[39] Gas-phase geometry optimized structures (Gaussian 03,[40] B3LYP/6-31G*) of compound **4**, which is the tris[(1*H*-pyrazol-1-yl)methyl] derivative (a motif based on Table 1, entry 3), convey the idea graphically (Figure 2, b). Each of the three pyrazoles can participate in 7MHB with exactly one neighboring OH; consequently, two conformations of similar energy result (*syn* and *anti*, with the *anti* conformer being more stable by 0.79 kcal mol^{-1}). Each conformer should exist as a racemate (*syn*/*syn'* and *anti*/*anti'*, not shown) in solution whereby the enantiomers differ in their H-bond directionality (when viewed from a common perspective). Although beyond the scope of this paper, the bowl-shaped *syn*/*syn'* conformer is particularly appealing for molecular recognition applications. Similar conformational considerations are expected for phloroglucinols **5** substituted with amide functions (a motif based on the results detailed in Table 1, entry 5).

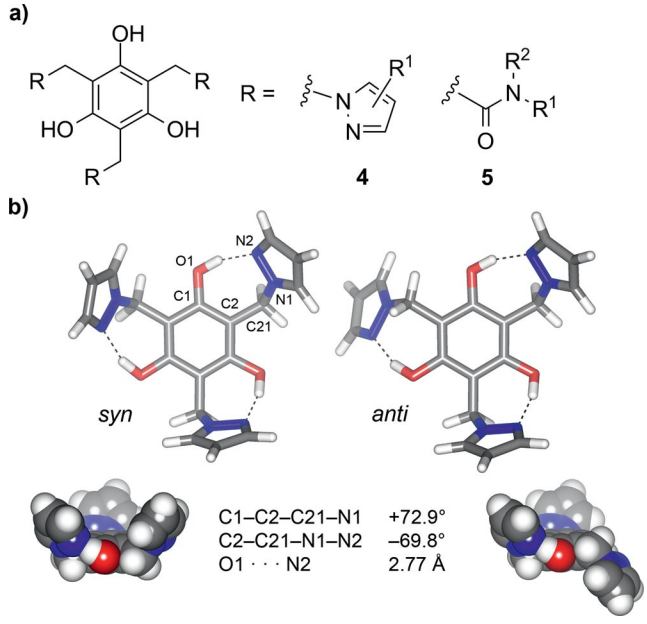

Figure 2. (a) Two classes of phloroglucinol model compounds considered experimentally in this work, each capable of three intramolecular 7MHB interactions; R^1 = H, alkyl, or aryl. (b) The geometry-minimized (B3LYP/6-31G*) *syn* and *anti* conformations of **4** (where R^1 = H). Only one enantiomer of each conformation is shown. Inset: Edge-on views of the conformations in CPK format.

Model Compound Synthesis

Two tris[(1*H*-pyrazol-1-yl)methyl] phloroglucinol derivatives **4** could be prepared (Table 4) through a two-step pro-

cedure from known 1,3,5-tris(bromomethyl)-2,4,6-trimethoxybenzene (**6**).[5a] Three-fold nucleophilic substitution with pyrazole (Table 4, entry 1) or 3,5-dimethylpyrazole (entry 2), both commercially available, provided trimethoxy derivatives **7a** and **7b** in moderate yield, respectively. Subsequent demethylation using BBr_3 at low temperature provided the phloroglucinol targets **4a** and **4b** in excellent yield. To generate a small library of model compounds **5**, we have capitalized on the versatile aminolysis chemistry of benzotrifuranone (BTF) **8**[5e–5g] (Table 5). Shown is the treatment of BTF with various aliphatic (**a**–**e**) and one aromatic (**f**) amines; the former include primary (**a**), branched/chiral (**b**), secondary acyclic (**c**), and secondary cyclic (**d** and **e**) derivatives that subtly vary the H-bond accepting ability of the amide carbonyl. These eight compounds, together with related phloroglucinols reported in our previous work, are sufficient to fully probe 7MHB spectroscopically (see below).

Table 4. Preparation of tris[(1*H*-pyrazol-1-yl)methyl] phloroglucinol derivatives **4**.

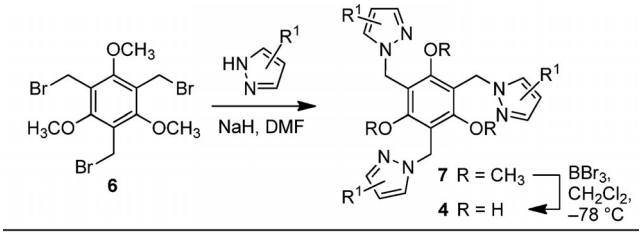

Entry	Pyrazole	% yield **7**	% yield **4**
a		68	98
b	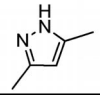	60	84

Table 5. Preparation of tris(acetamido)phloroglucinol model compounds through aminolysis of benzotrifuranone (BTF) **8**.

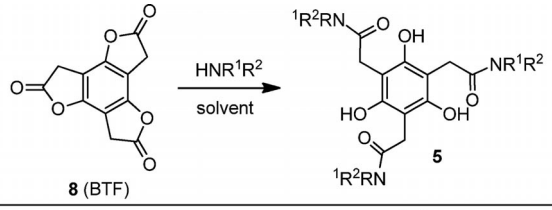

Entry	NR^1R^2	% yield	Entry	NR^1R^2	% yield
a	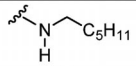	80	**d**	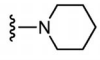	65
b	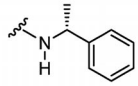	89	**e**	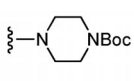	93
c		78	**f**	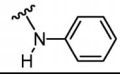	quant

7MHB in Solution; ^{1}H NMR Analysis of 4 and 5

The ^{1}H NMR spectra of **4** and **5** in $CDCl_3$ (Table 6, entries 2–9) all show relatively sharp phenolic OH resonances far downfield of the equivalent signal for persubstituted phloroglucinols that lack 7MHB capability (Table 6, entry 1). It is worth noting that in all cases the spectra are consistent with time-averaged C_3-symmetry in solution; the *syn* and *anti* forms (Figure 2) rapidly interconvert on the ^{1}H NMR time-scale at ambient temperature. Beginning with the pyrazoles (Table 6, entries 2 and 3), the chemical shift (δ_{OH}) of **4a** (entry 2) is both concentration independent (from 0.4–10 mM; see the Supporting Information for details) and similar to the values identified for the parent motif from the literature (Table 3, entry 3). The δ_{OH} value expectedly shifts downfield from **4a** (by 0.5 ppm) for the more electron rich (and more basic) 3,5-dimethylpyrazole derivative **4b** (Table 6, entry 3). A variable temperature ^{1}H NMR experiment with **4a** conducted from 223–283 K (see the Supporting Information for details) further confirms (a) the low barrier for conformational interconversion and (b) persistent intramolecular hydrogen bonding with a typical[2b] $\Delta\delta_{OH}/\Delta T$ value of -4.5×10^{-3} ppm/K.

Table 6. ^{1}H NMR spectroscopic data (δ_{OH}, $CDCl_3$) for **4** and **5**, and related phloroglucinols.[a]

Entry	Phloroglucinol	δ_{OH} ($CDCl_3$) [ppm]
1	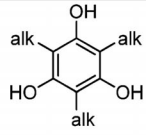	4.6[5d]
2	**4a**	10.9 (0.40 mM)
		10.9 (2.0 mM)
		10.9 (10 mM)[b]
3	**4b**	11.3
4	**5a**	10.2
5	**5b**	10.1 (0.40 mM)
		10.1 (2.0 mM)
		10.1 (10 mM)
		10.1 (50 mM)
6	**5c**	11.0
7	**5d**	10.7
8	**5e**	10.4
9	**5f**	9.76[5b]
10	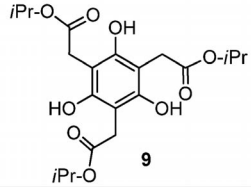	8.46[5d]

[a] Unless otherwise indicated, the solution concentration was 1–10 mM and spectra were recorded at ambient temperature. [b] The OH resonance at 50 mM is significantly broadened and is not reported.

Given the weaker basicity of the amide carbonyl (pyrazole pK_a = 2.5; *N*-methylacetamide pK_a = –0.4[41]), δ_{OH} for **5** (Table 6, entries 4–9) is generally upfield of **4** and the

values fall within the range established by the parent compounds in Table 3 (entry 5). Again, the chemical shifts are concentration independent (from 0.4–50 mM; see the Supporting Information for details) and the trends as R^1/R^2 (Table 5) are varied can be rationalized on the basis of subtle changes in carbonyl basicity. For example, δ_{OH} of the tertiary amides **5c**–**e** are downfield of the secondary amides **5a** and **5b**. Likewise, the Boc-protected piperazine ring of **5e** results in a weakening (via an inductive and/or transannular effect) of the intramolecular 7MHB and an upfield shift of δ_{OH} relative to piperidine **5d**. Lastly, aromatic amide **5f** shows the weakest H-bond, a result not predicted by pK_a values determined in water [i.e., *N*-methylacetamide (pK_a = –0.6); acetanilide (pK_a = 0.5)[37]]. The final entry in Table 6 includes known[5d] isopropyl acetate derivative **9**; the δ_{OH} value (δ = 8.46 ppm) is consistent with the weak basicity of the ester carbonyl versus the amides of the other entries (i.e., isopropyl acetate $pK_a \approx -3.5$[42]).

7MHB in the Solid State; X-ray Crystal Analysis of 4a and 5b

A single crystal of **4a** could be obtained by slowly diffusing pentane into its chloroform solution (Figure 3). X-ray analysis nicely confirms intramolecular 7MHB; related structural parameters are summarized in Table 7 and are in accordance with the values reported in Table 1 (entry 3). Molecule **4a** adopts the racemic *anti* conformation (as *anti* and *anti'*) in the solid phase. It is likely that the C_1-symmetric *anti* conformers can pack more efficiently than the C_3-symmetric *syn* conformers; for the former, the molecules pack into dimeric units (Figure 3, b) that are stabilized by

Table 7. 7MHB geometry of **4a** and **5b** from X-ray crystallography (lengths are given in Å units, angles in degree).[a]

Parameter	4a	Parameter	5b
O1···N2	2.7193(16)	O1···O4	2.628(3)
O2···N4	2.6884(16)	O2···O5	2.613(4)
O3···N6	2.7445(16)	O3···O6	2.666(4)
C1–C2–C21–N1	+73.13(16)	C1–C2–C21–C22	+68.4(4)
C3–C4–C41–N3	–70.10(16)	C3–C4–C41–C42	–69.4(4)
C5–C6–C61–N5	+75.94(16)	C5–C6–C61–C62	–71.9(4)
C2–C21–N1–N2	–68.58(16)	C2–C21–C22–O4	–65.7(4)
C4–C41–N3–N4	+67.92(15)	C4–C41–C42–O5	+59.4(4)
C6–C61–N5–N6	–68.14(16)	C6–C61–C62–O6	+55.4(4)

[a] Standard deviations are shown in parentheses. Additional crystallographic details are provided in the Exp. Sect. and Supporting Information. For **5b**, only the values for one of the two molecules from the unit cell are provided.

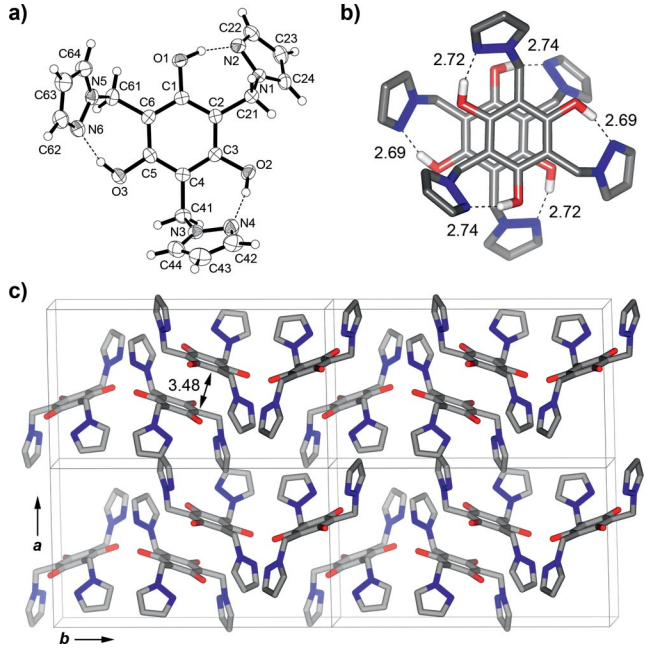

Figure 3. X-ray crystal structure of **4a**: (a) ORTEP plot (*anti* conformer, thermal ellipsoids shown at the 50% probability level); (b) top view of a dimeric unit formed from enantiomeric *anti* conformers of **4a** (*anti* and *anti'*) in the crystal lattice; (c) crystal packing of **4a** viewed along the *c* axis. H-bonds are shown as dashed lines. H-bond (N···O) and π-stacking (plane-to-plane) distances are given in Å. Atom colors: C, gray; H, white; N, blue; O, red.

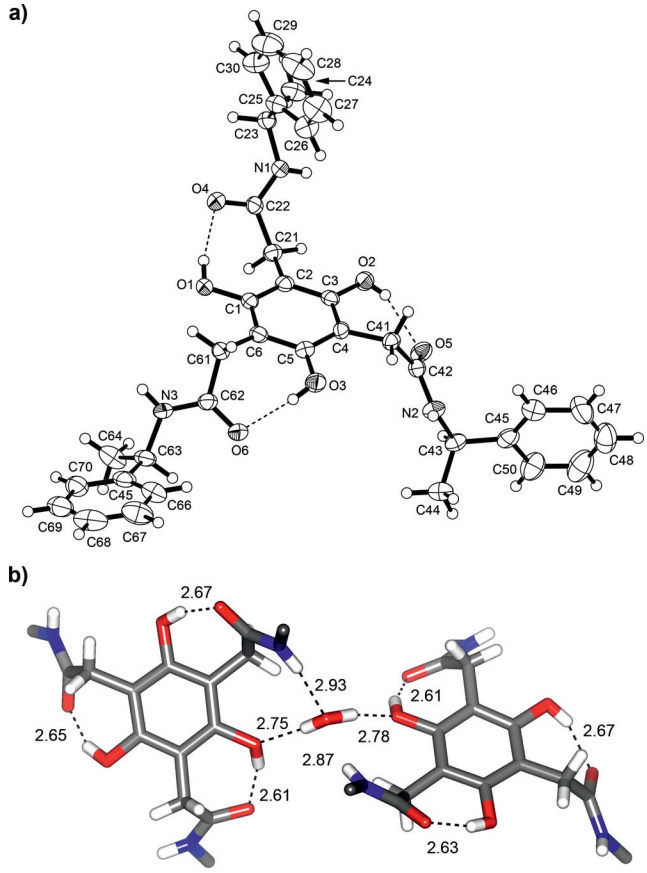

Figure 4. The X-ray crystal structure of **5b**: (a) ORTEP plot (*anti* conformer, thermal ellipsoids shown at the 50% probability level); (b) the unit cell including one water of crystallization (some atoms have been omitted for clarity). H-bonds are shown as dashed lines and H-bond lengths (O···O and N···O) are given in Å. Atom colors: C, gray; H, white; N, blue; O, red.

π–π interactions (the π-stacking distance is 3.48 Å). In the crystal packing, the *anti* and *anti′* conformers are found to array alternately (Figure 3, c) as viewed along the *c* axis. It is worth noting that the DFT calculated torsion angles and H-bond lengths for **4a** *anti* (Figure 2, b) agree excellently with the X-ray data presented in Table 7 within 0.3° and 0.5 Å, respectively.

A single crystal of **5b** could be obtained by slow evaporation of its ethyl acetate solution. In the X-ray structure (Figure 4, a), the expected H-bonds are found between the amide carbonyl oxygen atoms and the phenolic hydroxyl groups. Additionally, molecules of **5b** are organized into water-bridged dimers in the unit cell (Figure 4, b), an interesting assembly wherein all of the H-bonding sites of water are perfectly satisfied. It is also worth noting that only one conformation of the *anti* diastereomer is observed in the solid state (i.e., the diastereomeric *syn*, *syn′*, and *anti′* forms are not observed). The result contrasts with the crystal structure of compound **4a** wherein both the *anti* and *anti′* forms are present in the solid state. For **5b**, the peripheral stereogenic centers ultimately influence the H-bonding rotational sense at the phloroglucinol core.

Conclusions

A thorough search of the Cambridge Structural Database (CSD) has revealed that phenolic OH groups faithfully participate in intramolecular seven-membered hydrogen bonding (7MHB) arrangements when a suitable H-bond acceptor atom (X, Figure 1) is flexibly attached to the aromatic ring at C2. A number of common functional groups − amides, heterocycles, phosphane oxides, ketones, etc. − can serve as acceptors in this motif, and the resulting H-bond geometries closely match γ-turns that are well-studied in peptides. The contacts persist in organic solution (e.g., $CDCl_3$) and are readily inferred from published ^1H NMR spectroscopic data; the phenolic OH resonance is generally significantly deshielded (appearing between 7–13 ppm).

Persubstituted phloroglucinol derivatives **4** and **5** have been prepared as model compounds to characterize intramolecular 7MHB in the context of designed molecular systems. Two of the motifs identified from the CSD have been easily extended to this platform to produce scaffolds that are conformationally rigidified through a cyclic array of three intramolecular H-bonds. Two low-energy conformations, *syn* and *anti*, result when all the H-bond donors and acceptors are satisfied (based on DFT calculations). The H-bonding for **4** and **5** persists in both the solid state and solution. The *anti* form appears exclusively in the crystal, likely as a consequence of packing given the predicted similar energies of the two forms, although both the *syn* and *anti* forms are accessible in solution where they rapidly interconvert at ambient temperature.

Intramolecular seven-membered H-bonds are considered "weak" and are therefore typically overlooked in the design of conformationally-biased molecular hosts or catalysts. The demonstrated persistence of the seven-membered intramolecular H-bonds described here (and nine-membered intramolecular H-bonds described elsewhere[43]) should be useful for molecular architecture design because, unlike intramolecular five- and six-membered HB arrangements, larger rings stabilize nonplanar conformations that are potentially more suitable for molecular recognition applications.

Experimental Section

General: Reagents and solvents were purchased from commercial sources and used without further purification unless otherwise specified. THF, CH_2Cl_2, and DMF were degassed in 20 L drums and passed through two sequential purification columns (activated alumina; molecular sieves for DMF), under a positive argon atmosphere. Thin-layer chromatography (TLC) was performed on SiO_2-60 F254 aluminum plates with visualization by UV light or staining. Flash column chromatography was performed using Purasil SiO_2-60, 230–400 mesh from Whatman. ^1H and ^{13}C NMR spectra were recorded with Varian Mercury 300, Varian Gemini 300, or Varian VXR300 spectrometers (300 and 75 MHz) or with an Inova2 spectrometer (500 and 125 MHz). Chemical shifts (δ) are given in parts per million (ppm) relative to TMS and referenced to residual protonated solvent ($CDCl_3$: δ_H = 7.27 ppm, δ_C = 77.00 ppm. CD_3CN: δ_C = 118.70 ppm; [D_6]DMSO: δ_C = 39.51 ppm). Abbreviations used are: s (singlet), d (doublet), t (triplet), q (quartet), quin (quintet), hept (heptet), br (broad), and m (multiplet). ESI-TOF-MS spectra were recorded with an Agilent 6210 TOF spectrometer. CI-MS spectra were recorded with a Thermo Scientific Trace GC DSQ (single quadrupole) spectrometer. Compounds **6**[5a] and **8**[5e–5g] were prepared as described in the literature.

X-ray Crystal Structure Determination and Refinement: Data were collected at 173 K with a Siemens SMART PLATFORM equipped with a CCD area detector and a graphite monochromator utilizing Mo-K_α radiation (λ = 0.71073 Å). Cell parameters were refined by using up to 8192 reflections. A full sphere of data (1850 frames) was collected using the ω-scan method (0.3° frame width). The first 50 frames were remeasured at the end of data collection to monitor instrument and crystal stability (maximum correction on I was < 1%). Absorption corrections by integration were applied based on measured indexed crystal faces.

The structures were solved by the Direct Methods in *SHELXTL6*,[44] and refined using full-matrix least-squares on F^2. The non-H atoms were treated anisotropically, whereas the hydrogen atoms were calculated in ideal positions and were riding on their respective carbon atoms. For **4a**, a total of 257 parameters were refined in the final cycle of refinement using 3670 reflections with $I > 2\sigma(I)$ to yield R_1, wR_2, and S (goodness of fit) as 3.71%, 8.98%, and 0.953, respectively. For **5b**, the asymmetric unit consists of two molecules linked together by a water molecule through H-bonding. Here, a total of 876 parameters were refined in the final cycle of refinement using 8104 reflections with $I > 2\sigma(I)$ to yield R_1, wR_2, and S (goodness of fit) as 6.16%, 13.08%, and 0.933, respectively. The refinements were carried out by minimizing the wR_2 function using F^2 rather than F values. R_1 is calculated to provide a reference to the conventional R value but its function is not minimized. Further crystallographic parameters are provided in Table 8.

Table 8. Crystal data and structure refinement for **4a** and **5b**.

	4a	**5b**
Empirical formula	$C_{18}H_{18}N_6O_3$	$C_{72}H_{80}N_6O_{13}$
Formula weight	366.38	1237.42
Crystal system	monoclinic	orthorhombic
Space group	$P2_1/c$	$P2_12_12_1$
a [Å]	10.8634(8)	16.2768(2)
b [Å]	18.1231(13)	17.0749(11)
c [Å]	8.9672(7)	23.18(15)
α [°]	90	90
β [°]	104.052(1)	90
γ [°]	90	90
V [Å^3]	1712.6(2)	6442.3(7)
Z	4	4
$\rho_{calcd.}$ [g cm^{-3}]	1.421	1.276
Crystal size [mm]	0.32 × 0.23 × 0.18	0.19 × 0.16 × 0.15
Independent reflections	3670	14476
Index ranges	$-11 \le h \le 14$	$-11 \le h \le 21$
	$-13 \le k \le 23$	$-21 \le k \le 21$
	$-9 \le l \le 11$	$-27 \le l \le 29$
Parameters	257	876
F (000)	768	2632
Goodness-of-fit (on F^2)	0.953	0.933
R_1 based on F [$I > 2\sigma(I)$]	0.0371	0.0616
wR_2 based on F [$I > 2\sigma(I)$]	0.0898	0.1308

CCDC-874426 (for **4a**) and -874427 (for **5b**) contain the supplementary crystallographic data for this paper. These data can be obtained free of charge from The Cambridge Crystallographic Data Centre via www.ccdc.cam.ac.uk/data_request/cif.

1,1′,1′′-[(2,4,6-Trimethoxybenzene-1,3,5-triyl)tris(methylene)]tris-(1*H*-pyrazole) (7a): To a suspension of NaH (60% in mineral oil, 0.32 g, 7.9 mmol) and anhydrous DMF (30 mL) in a dry flask was added pyrazole (0.53 g, 7.4 mmol), after which the mixture was heated to 50 °C for 1 h. After cooling to room temperature, **6** (1.0 g, 2.2 mmol) was dissolved in a small amount of anhydrous DMF and slowly added to the stirring solution. Upon completion of addition, the mixture was warmed to 50 °C for 12 h. After cooling to room temperature, the mixture was carefully poured into water (40 mL), and extracted with ethyl acetate (3 × 50 mL). The organic layers were combined, dried with $MgSO_4$, and concentrated to a crude oil. Flash chromatography (EtOAc/hexanes, 1:5) afforded **7a** (0.62 g, 68%) as a white solid: ^{1}H NMR (300 MHz, $CDCl_3$): δ = 3.60 (s, 9 H), 5.37 (s, 6 H), 6.23 [t, $^3J_{H,H}$ = 2.1 Hz, 3 H], 7.45 (d, $^3J_{H,H}$ = 2.4 Hz, 3 H), 7.47 (d, $^3J_{H,H}$ = 1.8 Hz, 3 H) ppm. ^{13}C NMR (75 MHz, $CDCl_3$): δ = 45.4, 62.4, 105.4, 120.5, 129.2, 138.8, 160.3 ppm. HRMS (ESI-TOF): calcd. for $C_{21}H_{24}N_6O_3Na$ [M + Na]$^+$ 431.1802; found 431.1798.

1,1′,1′′-[(2,4,6-Trimethoxybenzene-1,3,5-triyl)tris(methylene)]tris-(3,5-dimethyl-1*H*-pyrazole) (7b): This compound was prepared analogously to **7a** using NaH (60% in mineral oil, 0.470 g, 11.8 mmol), 3,5-dimethylpyrazole (1.06 g, 11.1 mmol), and **6** (1.50 g, 3.36 mmol). Flash chromatography using ethyl acetate/hexanes (2:1) afforded **7b** (1.0 g, 60%) as a white solid: ^{1}H NMR (300 MHz, $CDCl_3$): δ = 2.15 (s, 9 H), 2.24 (s, 9 H), 3.47 (s, 9 H), 5.12 (s, 6 H), 5.76 (s, 3 H) ppm. ^{13}C NMR (75 MHz, CD_3CN): δ = 11.7, 14.0, 43.0, 62.9, 105.8, 122.5, 141.0, 147.7, 160.9 ppm. HRMS (ESI-TOF): calcd. for $C_{27}H_{37}N_6O_3$ [M + H]$^+$ 493.2922; found 493.2917.

2,4,6-Tris[(1*H*-pyrazol-1-yl)methyl]benzene-1,3,5-triol (4a): To a solution of **7a** (0.608 g, 1.66 mmol) and anhydrous dichloromethane (17 mL) at –78 °C in a dry flask equipped with a stirrer was added BBr_3 (5.84 g, 23.3 mmol). After 1 h, the mixture was allowed to gradually warm to room temperature and stirred overnight. After cooling to 0 °C, the reaction was quenched by dropwise addition of cold saturated aqueous $NaHCO_3$ until gas evolution ceased. The reaction mixture was then poured into saturated aqueous $NaHCO_3$ and extracted with dichloromethane (3 × 30 mL). The organic layers were combined, washed with brine, dried with $MgSO_4$, and concentrated under reduced pressure to afford **4a** (0.60 g, 98%) as a white solid. ^{1}H NMR (300 MHz, $CDCl_3$): δ = 5.38 (s, 6 H), 6.21 (t, $^3J_{H,H}$ = 2.1 Hz, 3 H), 7.49 (d, $^3J_{H,H}$ = 2.1 Hz, 3 H), 7.56 (d, $^3J_{H,H}$ = 2.1 Hz, 3 H), 10.90 (s, 3 H) ppm. ^{13}C NMR (125 MHz, [D$_6$]DMSO): δ = 44.6, 104.9, 105.3, 129.9, 138.2, 155.8 ppm. HRMS (ESI-TOF): calcd. for $C_{18}H_{18}N_6O_3Na$ [M + Na]$^+$ 389.1333; found 389.1336.

2,4,6-Tris[(3,5-dimethyl-1*H*-pyrazol-1-yl)methyl]benzene-1,3,5-triol (4b): Prepared analogously to **4a** using **7b** (0.50 g, 1.01 mmol) and BBr_3 (3.56 g, 14.2 mmol). The product **4b** (0.38 g, 84%) was isolated as a white solid. ^{1}H NMR (300 MHz, $CDCl_3$): δ = 2.16 (s, 9 H), 2.38 (s, 9 H), 5.20 (s, 3 H), 5.70 (s, 3 H), 11.33 (br. s, 3 H) ppm. ^{13}C NMR (75 MHz, $CDCl_3$): δ = 10.8, 13.2, 41.8, 104.6, 105.9, 139.5, 146.7, 156.0 ppm. HRMS (ESI-TOF): calcd. for $C_{24}H_{30}N_6O_3Na$ [M + Na]$^+$ 473.2272; found 473.2288.

2,2′,2′′-(2,4,6-Trihydroxybenzene-1,3,5-triyl)tris(*N*-hexylacetamide) (5a): To a solution of **8** (100 mg, 0.406 mmol) in THF (15 mL) was added *n*-hexylamine (410 mg, 4.06 mmol) and the resulting solution was stirred overnight. The solvent was then evaporated and the residue was taken up in EtOAc (30 mL), washed with 0.1 M HCl, water, and brine sequentially, and dried with Na_2SO_4. The solvent was removed and the residue was purified by flash column chromatography (EtOAc/hexanes, 2:5) to yield **5a** (179 mg, 80%) as an off-white solid. ^{1}H NMR (300 MHz, $CDCl_3$): δ = 0.88 (t, $^3J_{H,H}$ = 6.6 Hz, 9 H), 1.23–1.34 (m, 18 H), 1.43–1.58 (m, 6 H), 3.21 (q, $^3J_{H,H}$ = 6.9 Hz, 6 H), 3.60 (s, 6 H), 6.18 (t, $^3J_{H,H}$ = 5.8 Hz, 3 H), 10.19 (s, 3 H) ppm. ^{13}C NMR (75 MHz, $CDCl_3$): δ = 13.9, 22.5, 26.5, 29.1, 31.3, 40.0, 103.1, 153.8, 174.6 ppm. HRMS: calcd. for $C_{30}H_{51}N_3O_6Na$ [M + Na]$^+$ 614.4140; found 614.4147.

2,2′,2′′-(2,4,6-Trihydroxybenzene-1,3,5-triyl)tris{*N*-[(*R*)-1-phenylethyl]acetamide} (5b): Prepared similarly to **5a** using **8** (25.0 mg, 0.102 mmol) and (*R*)-(+)-α-methylbenzylamine (40.6 mg, 0.335 mmol) in DMF (3 mL). In this case, the reaction was performed beginning at 0 °C and then warmed to room temp. and stirred overnight. The crude product (62 mg, quant) was purified by flash column chromatography (acetone/CH_2Cl_2, 10%) to give **5b** (55 mg, 89%) as a brownish solid. $[\alpha]_D^{23.7}$ = +42.9 (*c* = 0.91, $CHCl_3$). ^{1}H NMR (300 MHz, $CDCl_3$): δ = 1.49 (d, $^3J_{H,H}$ = 6.9 Hz, 9 H), 3.56 (d, $^2J_{H,H}$ = 13.8 Hz, 3 H), 3.66 (d, $^2J_{H,H}$ = 13.8 Hz, 3 H), 5.01 (m, 3 H), 6.42 (m, 3 H, NH), 7.22–7.37 (m, 15 H), 10.07 (s, 3 H, OH) ppm. ^{13}C NMR (75 MHz, $CDCl_3$): δ = 21.8, 32.6, 49.5, 103.0, 126.0, 127.5, 128.7, 142.4, 153.9, 173.9 ppm. HRMS (CI): calcd. for $C_{36}H_{40}N_3O_6$ [M + H]$^+$ 610.2917; found 610.2924.

2,2′,2′′-(2,4,6-Trihydroxybenzene-1,3,5-triyl)tris(*N*,*N*-diethylacetamide) (5c): Prepared analogously to **5a** using **8** (80.0 mg, 0.325 mmol) and *N*,*N*-diethylamine (237 mg, 3.25 mmol) in THF (10 mL). The product **5c** (118 mg, 78%) was obtained after purification by flash column chromatography (EtOAc/hexanes, 1:3). ^{1}H NMR (300 MHz, $CDCl_3$): δ = 1.12 (t, $^3J_{H,H}$ = 7.2 Hz, 9 H), 1.27 (t, $^3J_{H,H}$ = 7.0 Hz, 9 H), 3.36 (q, $^3J_{H,H}$ = 7.3 Hz, 6 H), 3.67 (q, $^3J_{H,H}$ = 7.3 Hz, 6 H), 3.77 (s, 6 H), 11.00 (s, 3 H) ppm. ^{13}C NMR (75 MHz, $CDCl_3$): δ = 12.9, 14.6, 28.7, 41.1, 43.5, 102.0, 154.7, 174.3 ppm. HRMS (ESI-TOF): calcd. for $C_{24}H_{40}N_3O_6$ [M + H]$^+$ 466.2912; found 466.2925.

2,2′,2′′-(2,4,6-Trihydroxybenzene-1,3,5-triyl)tris[1-(piperidin-1-yl)-ethanone] (5d): Prepared analogously to **5a** using **8** (80 mg,

0.32 mmol) and piperidine (272 mg, 3.20 mmol) in acetone (10 mL). The product **5d** (106 mg, 65%) was obtained after purification by flash column chromatography (EtOAc/hexanes, 1:3). ^{1}H NMR (500 MHz, $CDCl_3$): δ = 1.50–1.57 (m, 6 H), 1.58–1.68 (m, 12 H), 3.54 (t, $^3J_{H,H}$ = 5.6 Hz, 6 H), 3.79 (s, 6 H), 3.83 (t, $^3J_{H,H}$ = 5.5 Hz, 6 H), 10.65 (s, 3 H) ppm. ^{13}C NMR (125 MHz, $CDCl_3$): δ = 24.4, 25.5, 26.5, 28.5, 43.3, 48.3, 102.0, 154.6, 172.8 ppm. HRMS (ESI-TOF): calcd. for $C_{27}H_{40}N_3O_6$ $[M + H]^+$ 502.2912; found 502.2916.

Tri-*tert*-butyl 4,4′,4′′-[2,2′,2′′-(2,4,6-Trihydroxybenzene-1,3,5-triyl)-tris(acetyl)]tris-(piperazine-1-carboxylate) (5e): Prepared analogously to **5a** using **8** (80 mg, 0.32 mmol) and mono-Boc-protected piperazine (300 mg, 1.62 mmol) in THF (10 mL). The product **5e** (240 mg, 93%) was obtained after purification by flash column chromatography (EtOAc/hexanes, 2:3). ^{1}H NMR (500 MHz, $CDCl_3$): δ = 1.46 (m, 27 H), 3.39 (m, 6 H), 3.45 (m, 6 H), 3.58 (m, 6 H), 3.78 (s, 6 H), 3.88 (m, 6 H), 10.37 (s, 3 H) ppm. ^{13}C NMR (125 MHz, $CDCl_3$): δ = 28.3, 28.6, 42.0, 46.8, 80.3, 101.9, 154.4, 154.5, 173.3 ppm. HRMS (ESI-TOF): calcd. for $C_{39}H_{61}N_6O_{12}$ $[M + H]^+$ 805.4342; found 805.4355.

2,2′,2′′-(2,4,6-Trihydroxybenzene-1,3,5-triyl)tris(*N*-phenylacetamide) (5f): To a solution of **8** (150 mg, 0.610 mmol) in DMF (7 mL) was added aniline (283 mg, 3.00 mmol). The resulting solution was heated to 70 °C for 15 h and then cooled to room temperature. The reaction solution was poured into brine (50 mL) and extracted with EtOAc. The combined organic layers were washed with 1 M HCl and water, and then dried with Na_2SO_4. The solvent was removed and the residue was purified by flash column chromatography (EtOAc/hexanes, 1:3 to 1:1) to yield **5f** (247 mg, quant). The ^{1}H and ^{13}C NMR spectroscopic data match those reported in the literature.[5b]

Supporting Information (see footnote on the first page of this article): Additional NMR spectroscopic data including copies of ^{1}H and ^{13}C NMR spectra of all new compounds, additional graphical structures from Table 1 and Table 2, and computational details.

Acknowledgments

This work was financially supported by the National Science Foundation (NSF) (CAREER program, grant number CHE-0548003 and Foundation REU program, CHE-0139505) and the University of Florida. A. J. L. was supported by a University of Florida Alumni Graduate Fellowship and E. A. H. by the NSF and the UF University Scholars program. K. A. A. wishes to acknowledge the NSF and the University of Florida for funding of the purchase of the X-ray equipment. The authors also thank Matthew B. Baker and Raghida Bou Zerdan for contributing to the characterization aspects of this work.

[1] a) C. Toniolo, E. Benedetti, *Crit. Rev. Biochem. Mol. Biol.* **1980**, *9*, 1–44; b) G. D. Rose, L. M. Glerasch, J. A. Smith, in: *Adv. Protein Chem.*, vol. 37 (Eds.: J. T. E. C. B. Anfinsen, M. R. Frederic), Academic Press, **1985**, pp. 1–109; c) G. A. Jeffrey, W. Saenger, *Hydrogen Bonding in Biological Structures*, Springer, Berlin, **1991**; d) E. Vass, M. Hollósi, F. Besson, R. Buchet, *Chem. Rev.* **2003**, *103*, 1917–1954; e) M. Crisma, F. Formaggio, A. Moretto, C. Toniolo, *Biopolymers* **2006**, *84*, 3–12.

[2] a) S. H. Gellman, G. P. Dado, G. B. Liang, B. R. Adams, *J. Am. Chem. Soc.* **1991**, *113*, 1164–1173; b) G. P. Dado, S. H. Gellman, *J. Am. Chem. Soc.* **1993**, *115*, 4228–4245; c) B. W. Gung, Z. H. Zhu, D. Zou, B. Everingham, A. Oyeamalu, R. M. Crist, J. Baudlier, *J. Org. Chem.* **1998**, *63*, 5750–5761; d) A. I. Jiménez, G. Ballano, C. Cativiela, *Angew. Chem.* **2005**, *117*, 400; *Angew. Chem. Int. Ed.* **2005**, *44*, 396–399; e) P. K. Baruah, N. K. Sreedevi, R. Gonnade, S. Ravindranathan, K. Damodaran, H.-J. Hofmann, G. J. Sanjayan, *J. Org. Chem.* **2006**, *72*, 636–639; f) S. Chatterjee, P. G. Vasudev, K. Ananda, S. Raghothama, N. Shamala, P. Balaram, *J. Org. Chem.* **2008**, *73*, 6595–6606; g) X. Li, Y. D. Wu, D. Yang, *Acc. Chem. Res.* **2008**, *41*, 1428–1438; h) B. Kuhn, P. Mohr, M. Stahl, *J. Med. Chem.* **2010**, *53*, 2601–2611.

[3] a) J. Recker, D. J. Tomcik, J. R. Parquette, *J. Am. Chem. Soc.* **2000**, *122*, 10298–10307; b) R. P. Sijbesma, E. W. Meijer, *Chem. Commun.* **2003**, 5–16; c) A. J. Wilson, *Soft Matter* **2007**, *3*, 409–425; d) B. Gong, *Acc. Chem. Res.* **2008**, *41*, 1376–1386; e) Z. T. Li, *Prog. Chem.* **2011**, *23*, 1–12; f) G. Conn, S. Eisler, *Org. Lett.* **2011**, *13*, 5080–5083.

[4] M. K. Lindvall, K. Rissanen, J. M. L. Hakala, A. M. P. Koskinen, *Tetrahedron Lett.* **1999**, *40*, 7427–7430.

[5] a) H. Li, E. A. Homan, A. J. Lampkins, I. Ghiviriga, R. K. Castellano, *Org. Lett.* **2005**, *7*, 443; b) A. J. Lampkins, O. Abdul-Rahim, H. Li, R. K. Castellano, *Org. Lett.* **2005**, *7*, 4471–4474; c) A. J. Lampkins, O. Abdul-Rahim, R. K. Castellano, *J. Org. Chem.* **2006**, *71*, 5815–5818; d) A. J. Lampkins, Y. Li, A. Al Abbas, K. A. Abboud, I. Ghiviriga, R. K. Castellano, *Chem. Eur. J.* **2008**, *14*, 1452–1463; e) M. B. Baker, L. Yuan, C. J. Marth, Y. Li, R. K. Castellano, *Supramol. Chem.* **2010**, *22*, 789–802; f) M. B. Baker, I. Ghiviriga, R. K. Castellano, *Chem. Sci.* **2012**, *3*, 1095–1099; g) Y. Li, A. J. Lampkins, M. B. Baker, B. G. Sumpter, J. Huang, K. A. Abboud, R. K. Castellano, *Org. Lett.* **2009**, *11*, 4314–4317.

[6] T. F. Markle, J. M. Mayer, *Angew. Chem.* **2008**, *120*, 750; *Angew. Chem. Int. Ed.* **2008**, *47*, 738–740.

[7] D. Zhang, H. Aihara, T. Watanabe, T. Matsuo, H. Kawaguchi, *J. Organomet. Chem.* **2007**, *692*, 234–242.

[8] C. X. Yin, F. J. Huo, F. Gao, J. P. Guo, P. Yang, *Acta Crystallogr., Sect. E: Struct. Rep. Online* **2003**, *59*, O1740–O1741.

[9] I. Sylvestre, C. A. Kilner, M. A. Halcrow, *Acta Crystallogr., Sect. C: Cryst. Struct. Commun.* **2005**, *61*, o294–o296.

[10] T. Higgs, C. Carrano, *Eur. J. Org. Chem.* **2002**, 3632–3645.

[11] S. Scheuermann, T. Kretz, H. Vitze, J. Bats, M. Bolte, H. W. Lerner, M. Wagner, *Chem. Eur. J.* **2008**, *14*, 2590–2601.

[12] Z. Chu, W. Huang, H. Zhu, S. Gou, *J. Mol. Struct.* **2008**, *874*, 1–13.

[13] H.-B. Zhu, Z.-L. Chu, D.-H. Hu, W. Huang, S.-H. Gou, *Inorg. Chem. Commun.* **2007**, *10*, 362–366.

[14] Z.-L. Chu, H.-B. Zhu, D.-H. Hu, W. Huang, S.-H. Gou, *Cryst. Growth Des.* **2008**, *8*, 1599–1604.

[15] F. W. Goldberg, P. Magnus, R. Turnbull, *Org. Lett.* **2005**, *7*, 4531–4534.

[16] T. Focken, H. Hopf, V. Snieckus, I. Dix, P. Jones, *Eur. J. Org. Chem.* **2001**, 2221–2228.

[17] D. B. Ramachary, Y. V. Reddy, M. Kishor, *Org. Biomol. Chem.* **2008**, *6*, 4188–4197.

[18] A. B. Cooper, J. Wang, A. K. Saksena, V. Girijavallabhan, K. G. Ashit, C. Tze-Ming, A. T. McPhail, *Tetrahedron* **1992**, *48*, 4757–4766.

[19] F. Sugawara, S. Strobel, G. Strobel, R. D. Larsen, D. L. Berglund, G. Gray, N. Takahashi, S. J. Coval, T. J. Stout, J. Clardy, *J. Org. Chem.* **1991**, *56*, 909–910.

[20] B. a. Legouin, P. Uriac, S. Tomasi, L. c. Toupet, A. Bondon, P. van de Weghe, *Org. Lett.* **2009**, *11*, 745–748.

[21] J. C. Gallucci, R. R. Holmes, *Inorg. Chem.* **1980**, *19*, 3540–3541.

[22] X. Yu, T. J. Marks, *Organometallics* **2006**, *26*, 365–376.

[23] A. Matveeva, Z. Starikova, E. Matrosov, G. Bodrin, S. Matveev, E. Nifant′ev, *Russ. J. Inorg. Chem.* **2006**, *51*, 253–266.

[24] W. B. Chen, D. A. Parrish, J. R. Deschamps, A. Coop, *Helv. Chim. Acta* **2005**, *88*, 822–829.

[25] A. Mukhopadhyyay, S. K. Talapatra, A. K. Saha, P. K. Lala, S. K. Mazumdar, K. Bhattacharyya, *Acta Crystallogr., Sect. C: Cryst. Struct. Commun.* **1998**, *54*, 399–401.

[26] J. G. Luis, L. S. Andrés, A. Perales, *Tetrahedron* **1993**, *49*, 4993–5000.
[27] M. Schnabelrauch, A. Vasella, S. G. Withers, *Helv. Chim. Acta* **1994**, *77*, 778–799.
[28] A. Usman, I. A. Razak, H.-K. Fun, S. Chantrapromma, Y. Zhang, J.-H. Xu, *Acta Crystallogr., Sect. C: Cryst. Struct. Commun.* **2002**, *58*, o477–o479.
[29] G. Sartori, R. Maggi, F. Bigi, A. Arienti, C. Porta, G. Predieri, *Tetrahedron* **1994**, *50*, 10587–10596.
[30] M. Ogata, H. Matsumoto, K. Takahashi, S. Shimizu, S. Kida, M. Ueda, S. Kimoto, M. Haruna, *J. Med. Chem.* **1984**, *27*, 1142–1149.
[31] C. T. Chen, W. K. Chang, S. C. Sheu, G. H. Lee, T. I. Ho, Y. C. Lin, W. Yu, *J. Chem. Soc., Dalton Trans.* **1991**, 1569–1573.
[32] O. Munoz-Muniz, E. Juaristi, *Tetrahedron Lett.* **2003**, *44*, 2023–2026.
[33] B. Ledoussal, A. Gorgues, A. Le Coq, *Tetrahedron* **1987**, *43*, 5841–5852.
[34] P.-Y. Renard, P. Vayron, C. Mioskowski, *Org. Lett.* **2003**, *5*, 1661–1664.
[35] O. Muñoz-Muñiz, E. Juaristi, *Tetrahedron* **2003**, *59*, 4223–4229.
[36] H. C. Kolb, M. G. Finn, K. B. Sharpless, *Angew. Chem.* **2001**, *113*, 2056; *Angew. Chem. Int. Ed.* **2001**, *40*, 2004–2021.
[37] CRC Handbook of Chemistry and Physics. 92nd ed.; 2011–2012. http://www.hbcpnetbase.com/.
[38] F. Besseau, M. Lucon, C. Laurence, M. Berthelot, *J. Chem. Soc. Perkin Trans. 2* **1998**, 101–108.
[39] a) G. Hennrich, E. V. Anslyn, *Chem. Eur. J.* **2002**, *8*, 2219–2224; b) C. Moberg, *Angew. Chem.* **2006**, *118*, 4838; *Angew. Chem. Int. Ed.* **2006**, *45*, 4721–4723; c) G. V. Zyryanov, M. A. Palacios, P. Anzenbacher, *Angew. Chem.* **2007**, *119*, 7995; *Angew. Chem. Int. Ed.* **2007**, *46*, 7849–7852; d) C. Schmuck, M. Heller, *Org. Biomol. Chem.* **2007**, *5*, 787–791; e) D. J. Mahnke, R. McDonald, F. Hof, *Chem. Commun.* **2007**, 3738–3740; f) L. J. Prins, F. Mancin, P. Scrimin, *Curr. Org. Chem.* **2009**, *13*, 1050–1064; g) G. M. Dell'Anna, R. Annunziata, M. Benaglia, G. Celentano, F. Cozzi, O. Francesconi, S. Roelens, *Org. Biomol. Chem.* **2009**, *7*, 3871–3877; h) A. Barnard, S. J. Dickson, M. J. Paterson, A. M. Todd, J. W. Steed, *Org. Biomol. Chem.* **2009**, *7*, 1554–1561; i) M. Arunachalam, P. Ghosh, *Chem. Commun.* **2009**, 5389–5391; j) C. Nativi, O. Francesconi, G. Gabrielli, A. Vacca, S. Roelens, *Chem. Eur. J.* **2011**, *17*, 4814–4820; k) A. Ardá, F. J. Cañada, C. Nativi, O. Francesconi, G. Gabrielli, A. Ienco, J. Jiménez-Barbero, S. Roelens, *Chem. Eur. J.* **2011**, *17*, 4821–4829; l) F. Fabris, O. De Lucchi, I. Nardini, M. Crisma, A. Mazzanti, S. A. Mason, M.-H. Lemee-Cailleau, F. A. Scaramuzzo, C. Zonta, *Org. Biomol. Chem.* **2012**, *10*, 2464–2469; m) X. Wang, F. Hof, *Beilstein J. Org. Chem.* **2012**, *8*, 1–10.
[40] M. J. Frisch, G. W. Trucks, H. B. Schlegel, G. E. Scuseria, M. A. Robb, J. R. Cheeseman, J. A. Montgomery, T. Vreven Jr, K. N. Kudin, J. C. Burant, J. M. Millam, S. S. Iyengar, J. Tomasi, V. Barone, B. Mennucci, M. Cossi, G. Scalmani, N. Rega, G. A. Petersson, H. Nakatsuji, M. Hada, M. Ehara, K. Toyota, R. Fukuda, J. Hasegawa, M. Ishida, T. Nakajima, Y. Honda, O. Kitao, H. Nakai, L. X. M. Klene, J. E. Knox, H. P. Hratchian, J. B. Cross, C. Adamo, J. Jaramillo, R. Gomperts, R. E. Stratmann, O. Yazyev, A. J. Austin, R. Cammi, C. Pomelli, J. W. Ochterski, P. Y. Ayala, K. Morokuma, G. A. Voth, P. Salvador, J. J. Dannenberg, V. G. Zakrzewski, S. Dapprich, A. D. Daniels, M. C. Strain, O. Farkas, D. K. Malick, A. D. Rabuck, K. Raghavachari, J. B. Foresman, J. V. Ortiz, Q. Cui, A. G. Baboul, S. Clifford, J. Cioslowski, B. B. Stefanov, G. Liu, A. Liashenko, P. Piskorz, I. Komaromi, R. L. Martin, D. J. Fox, T. Keith, M. A. Al-Laham, C. Y. Peng, A. Nanayakkara, M. Challacombe, P. M. W. Gill, B. Johnson, W. Chen, M. W. Wong, C. Gonzalez, J. A. Pople, *Gaussian 03*, rev. E.01, Gaussian, Inc., Pittsburgh, PA, **2003**.
[41] H. M. Grant, P. Mctigue, D. G. Ward, *Aust. J. Chem.* **1983**, *36*, 2211–2218.
[42] D. G. Lee, M. H. Sadar, *J. Am. Chem. Soc.* **1974**, *96*, 2862–2867.
[43] Y. Yoshimi, H. Maeda, M. Hatanaka, K. Mizuno, *Tetrahedron* **2004**, *60*, 9425–9431.
[44] *SHELXTL6*, Bruker-AXS, Madison, Wisconsin, USA, **2000**.
Received: April 4, 2012
Published Online: ■

EurJOC European Journal of Organic Chemistry

The structural and spectroscopic consequences of seven-membered intramolecular hydrogen bonding of phenols have been elucidated through crystallographic database searching and model compound investigation. The resulting H-bond geometries closely match peptide γ-turns, and the interactions are persistent in both solution and the solid state.

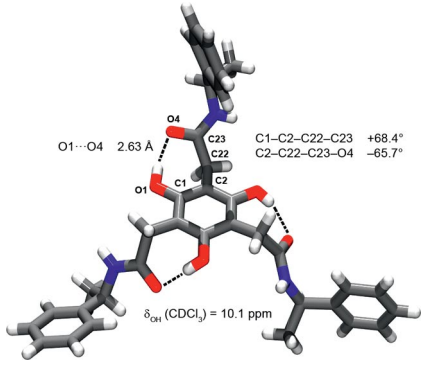

R. K. Castellano,* Y. Li, E. A. Homan, A. J. Lampkins, I. V. Marín, K. A. Abboud **1–11**

Seven-Membered Intramolecular Hydrogen Bonding of Phenols: Database Analysis and Phloroglucinol Model Compounds

Keywords: Conformation analysis / Crystal engineering / Hydrogen bonds / Solid-state structures / Supramolecular chemistry

